

# Training effect in Fe–Mn–Si shape-memory alloys

Y. WATANABE\*, Y. MORI, A. SATO

*Department of Materials Science and Engineering, Tokyo Institute of Technology, 4259 Nagatsuta, Midori-ku, Yokohama 227, Japan*

The training effect in Fe–Mn–Si shape-memory alloys has been examined by length change and electrical resistivity measurements. After 13 deformation–heating cycles, it was found that the major recovery took place at a temperature lower by 30 K than the first cycle. Simple thermal cycling also lowered the starting temperature of the reverse transformation and increased the finishing temperature. At the same time, the martensitic transformation temperature was found to increase significantly, for example by 35 K, at the 14th thermal cycle. The characteristics of shape-memory effect affected by development of the homogeneous and fine deformation structure by the thermal cycling are discussed in the light of the training effect.

## 1. Introduction

It is known that an Fe–Mn–Si alloy containing suitable amount of manganese and silicon exhibits a good shape-memory effect (SME) of a one-way type, governed by the f c c ( $\gamma$ )  $\rightleftharpoons$  h c p ( $\epsilon$ ) transformation [1–5]. For example, the alloy containing 31 wt % Mn and 6.5 wt % Si exhibits an SME greater than 99% upon deformation at any temperature between 4.2 and 300 K and subsequent heating above 500 K [2]. The origin of the SME is solely attributable to the generation of a particular type of Shockley partial dislocations, as has been demonstrated in the earlier works [1, 5].

The more popular and historical shape-memory alloys are Ni–Ti and copper-based alloys. These alloys, which have an ordered structure, show thermoelastic properties. It is also known that the SME characteristics of copper-based alloys are strongly affected by the prior deformation and heat treatment [6, 7]. For example, the starting temperature of the martensitic transformation,  $M_s$ , increases with the number of cycles and concurrently improves the SME property [7]. This is called a “training effect”.

In a recent study [8], the “training effect” has been noticed in the SME of a polycrystalline Fe–Mn–Si alloy by repeated deformation and heating cycles; similarly, in other iron-based alloys [9] governed by the  $\gamma \rightleftharpoons \epsilon$  martensitic transformation. The purpose of the present study was to determine whether such an effect also appears in a single crystal. It was expected that clearer information would be obtained by the use of a single crystal in discussing the origin of the training effect.

## 2. Experimental procedure

### 2.1. Deformation–heating cycles

A single-crystal rod of Fe–31 wt % Mn–6 wt % Si alloy was grown by the Bridgman method in an argon atmosphere. After homogenization treatment at 1453 K for 100 h, tensile specimens of a rectangular shape shown in Fig. 1 were cut by a wheel cutter. These specimens were annealed at 1273 K for 1 h and subsequently quenched into silicone oil at 473 K to avoid the occurrence of martensitic transformation during quenching. The composition of the single crystal specimens thus prepared varied from batch to batch by  $\sim 1$  wt % for the manganese content and  $\sim 0.5$  wt % for silicon, depending on the location of the single-crystal rod. After removing the surface oxide layers by electrolytic polishing, the rods were further annealed at 473 K for 20 min in order to eliminate  $\epsilon$ -martensite introduced during specimen preparation.

The crystallographic geometry of the specimen used in the cyclic deformation–heating tests is shown in Fig. 1a. The [414] tensile direction was chosen because the Schmid factor is 0.500 for the primary [121] ( $1\bar{1}1$ ) shear system and 0.385 for the secondary one. The surface plane ( $1\bar{8}1$ ) was chosen because the width of the specimen does not change for this geometry in the tensile test. Seven point markings were made using a microVickers hardness tester for length change measurements as shown in Fig. 1b. Tensile strain of 1%–6% was given at room temperature at a strain rate of  $3 \times 10^{-4} \text{ s}^{-1}$  with an Instron-type testing machine. After tensile deformation, the specimen was annealed at 673 K for 20 min in order to complete the

\*Present address: Department of Metallurgical Engineering, Hokkaido University, Kita-ku, Sapporo, Hokkaido 060, Japan.

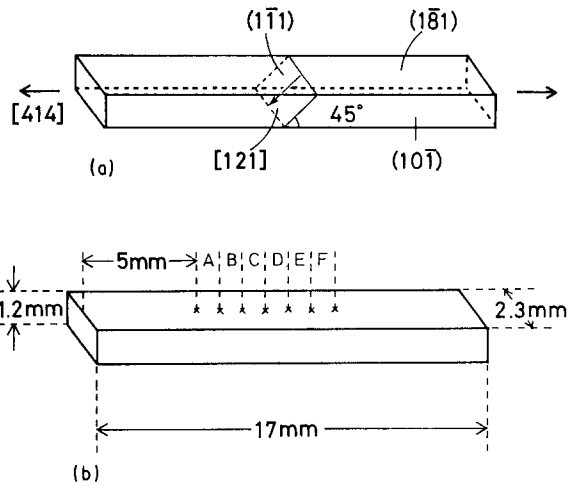


Figure 1 (a) Crystallographic geometry of the primary shear system expected to operate in the present specimen. (b) Location of indentation markings used for length change measurements.

$\epsilon \rightarrow \gamma$  reverse transformation. Length changes due to tensile deformation and heating cycles were measured by observing relative displacements between the Vickers markings under a precision machinery microscope after deformation and heating. The deformation–heating cycles were repeated 20 times for the same specimen.

In the different series of experiments, total length change was measured as a function of recovery temperature by repeated 1%–2% deformation given at 300 K and heating to either 523 or 693 K, and measuring the shrinkage fraction with respect to the elongation given at each cycle. The crystallographic orientation of the specimen used in this series of tests is the same as given in Fig. 1a.

## 2.2. Thermal cycles and electrical resistivity measurements

The polycrystalline specimens were prepared from a hot-rolled sheet for the simple thermal cycling tests without deformation. After removing the surface oxide layers by emery paper and electrolytic polishing, the specimens were annealed at 473 K for 30 min and air-cooled. The effect of thermal cycling on the transformation temperature was examined by measuring the electrical resistivity. The dimensions of the specimens used for this test were  $1.4 \times 0.3 \times 17 \text{ mm}^3$ . Electrical resistance was recorded as a function of temperature by a four-terminal d.c. current method. The temperature of the thermal cycling ranged between 77 and 500 K.

## 3. Results

### 3.1. Deformation–heating cycles and temperature of reverse transformation

The temperature dependence of a critical resolved shear stress (CRSS) measured on a single crystal is shown in Fig. 2. The data points, except B, in the figure were obtained on the same specimen by starting deformation at the highest temperature, 480 K, and repeat-

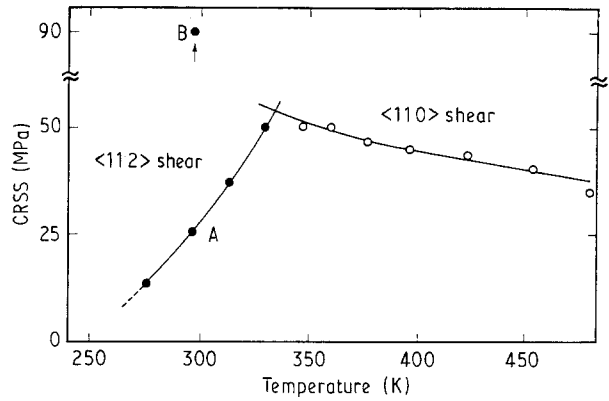


Figure 2 Temperature dependences of CRSSs resolved on  $\langle 112 \rangle \{111\}$  and  $\langle 110 \rangle \{111\}$  shear systems.

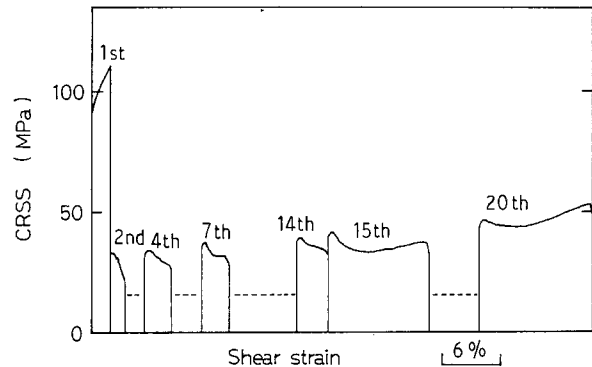


Figure 3 Stress–strain diagrams obtained at room temperature before and after repeated deformation–heating cycles. Cycle number: (○) 1, (△) 2, (□) 3, (◇) 4, (●) 8, (▲) 9, (■) 13.

ing it successively at a lower temperature. The temperature dependence is characterized by the evolution of a clear transition at about 330 K. The positive temperature dependence in Fig. 2 indicates that yielding occurs by  $\gamma \rightarrow \epsilon$  martensitic transformation below this temperature. On the other hand, yielding occurs by the usual slip above this temperature with normal temperature dependence. Fig. 3 shows the stress–strain diagrams obtained at room temperature after repeated heating cycles. As shown in the figure, 1%–2% tensile strain was given between the first and fourteenth tests and 5%–6% tensile strain was given between the fifteenth and twentieth tests. The data point B, marked by an arrow in Fig. 2, shows the yield stress obtained at the first tensile test shown in Fig. 3. This stress level is much higher than the yield stress obtained at room temperature (point A, Fig. 2) after the first deformation–heating cycle (Fig. 3). This indicates that the final annealing at 473 K before the deformation–heating cycle was not sufficient to eliminate  $\epsilon$  martensite introduced during specimen preparation.

Fig. 4 shows the effect of deformation–heating cycles on the shape recovery of the single crystals elongated along the [414] direction at room temperature. When the maximum heating temperature was set at 523 K, SME, which was nearly 100% in the initial few cycles, became incomplete with increasing number of cycles. At the same time, the starting temperature of

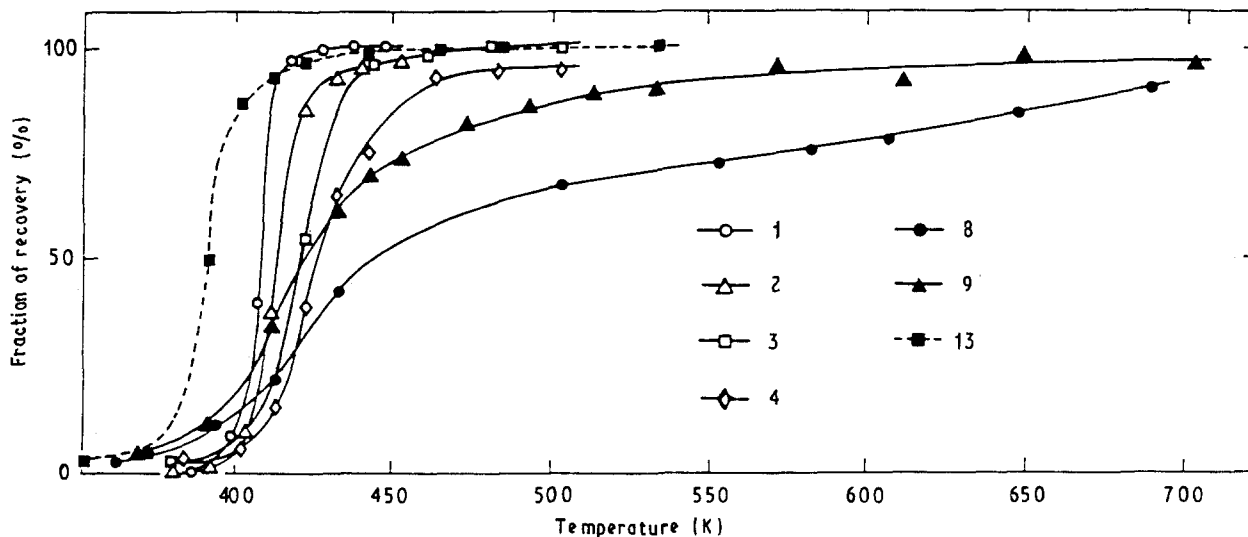


Figure 4 Fraction of recovery strain plotted against annealing temperature.

the reverse transformation,  $A_s$ , was lowered and the finishing temperature,  $A_f$ , was raised by the repeated deformation and heating cycles. This change was apparently caused by accumulation of residual  $\epsilon$  martensites and hence evolution of internal stress by the repeated deformation and insufficient recovery. The internal stress, which varies from place to place, may either suppress or assist the  $\epsilon \rightarrow \gamma$  reverse transformation depending on the sense of the stress, resulting in a lowering of  $A_s$  and increasing of  $A_f$ .

When the maximum heating temperature was raised to 693 K, the residual internal stress was released, thereby, recovering the original length. Upon further cycles with heating up to 693 K, a 100% SME was observed repeatedly. In the thirteenth cycle, recovery took place at a temperature lower by 30 K than the first cycle. The recovery was also completed in a much narrower temperature range. The trend that the cyclic treatment lowers the reverse transformation temperature is in agreement with the "training effect" found in polycrystals [8, 9].

### 3.2. Structural change due to deformation-heating cycles

Variation of local strains induced by repeated tensile deformation at different locations of specimens is shown in Fig. 5. In which A-F indicate the locations of the specimen shown in Fig. 1b. Tensile strain of 1%–2% was given at the first to fourteenth deformation-heating cycles. Deformations were not uniform in these cycles, as shown in Fig. 5. A tensile strain of 5%–6% was given at the fifteenth to twentieth deformation-heating cycles. Uniform deformation was gradually established by repetition of the deformation-heating cycles with a larger strain. Although the data are not shown, it should be noted that a complete shape-memory effect was obtained every time in these 20 cycles. Because the local strain at any location A-F did not exceed 10%, the complete shape recovery is a reasonable result for the [414] tensile tests. As previously demonstrated in the orientation

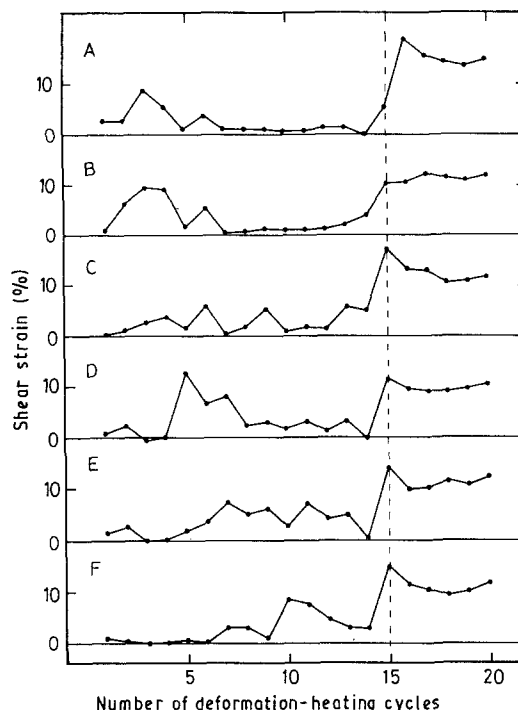


Figure 5 Variation of local strains induced by repeated tensile deformations at different locations of a specimen.

and strain dependences of SME [2], 10% elongation is the limiting strain to obtain a complete SME for the [414] tensile axis.

Another interesting point to be noted in Fig. 5 is that the region where larger deformation has taken place at a certain cycle, does not deform significantly in the following cycle as shown by the zigzag shape of the lines connecting data points. This means that the dislocations introduced in the deformed region do not necessarily contribute to the deformation in a significant manner in subsequent tests. In this way, the structure is homogenized by repetition of the deformation-heating cycle.

Surface morphology of the deformed and heated specimen is shown in Fig. 6. The microstructure of the

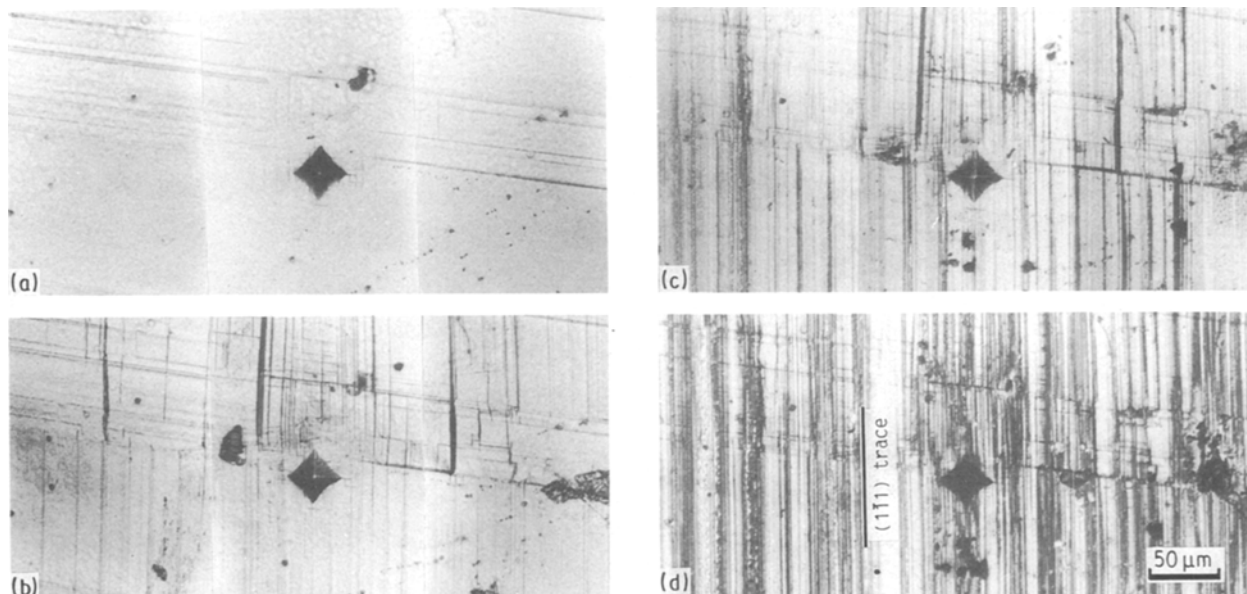


Figure 6 Optical micrographs taken on the  $(1\bar{8}1)$  surface of the present specimen: (a) before deformation, (b) after the first deformation, (c) after the third deformation, (d) after the seventh deformation.

specimen before the training cycle is shown in (a) and after the first, third and seventh cycles in (b–d), respectively. The pre-existing horizontal lines seen in the micrographs were introduced during specimen preparation. It is clearly demonstrated in Fig. 6b that the new shear bands formed along the vertical direction are mostly stopped at the pre-existing  $\epsilon$  martensites, causing an increase in the yield stress as shown by data point B in Fig. 2. Some of the pre-existing variants fade away with repeated deformation–heating cycles. Moreover, fresh  $\epsilon$  martensites increased in number to cover the entire area homogeneously after application of further deformation cycles. This structural change explains the recovery temperature shift found in Fig. 4, as discussed later.

### 3.3. Thermal cycles and electrical resistivity change

Fig. 7 shows the electrical resistivity versus temperature curves for a polycrystalline Fe–Mn–Si alloy. Arrows indicate the starting temperature of martensitic transformation,  $M_s$ , during simple cooling, and the temperature of major reverse transformation,  $T_R$ . It is seen that thermal cycling lowers  $T_R$ , for example by 30 K in the fourteenth run, but it raises the finishing temperature as observed in the deformation–heating cycles of single crystals shown in Fig. 4. In the fourteenth cycle, martensitic transformation took place at a temperature higher by 35 K than the first cycle. This temperature shift, as well as an increase in the electrical resistivity level and a decrease in the amount of resistivity hysteresis found in polycrystalline Fe–Mn–Si, may also be attributable to the structural change and the increase in the internal stress as mentioned previously in the work on single crystals.

## 4. Discussion

A training effect in an Fe–Mn–Si shape memory alloy has been reported as a useful method to improve the

SME property of a hot-rolled polycrystalline Fe–Mn–Si alloy [8]. However, the reason why the property is improved in this alloy has not been discussed in detail. As seen in the single crystalline work, Fig. 5, it is interesting that the amount of strain varies from place to place and that the undeformed region tends to deform preferentially in the following deformation–heating cycle, thus, exhibiting zigzag curves shown in Fig. 5. This is an indication that repetition of the deformation–heating cycle contributes to the homogenization of the internal structure. This homogenization is apparently achieved by introduction of new  $\epsilon$ -martensites distributed in fine scale, as shown in the surface morphology of Fig. 6. Corresponding to this structural change, the reverse transformation temperature is found to decrease by a substantial amount, as shown in Fig. 4, and similarly the electrical resistivity changes in a polycrystalline specimen upon thermal cycling, as shown in Fig. 7. Homogenization and refinement of the internal structure also contribute to the quick recovery of the shape change upon heating as indicated in the isochronal heating curves of Fig. 4.

When this characteristic change caused by the thermal cycling is inferred as due to the training effect reported in polycrystalline alloys, the occurrence of the simultaneous shape recovery in various grains, which may be completed in a narrower temperature range, is considered to contribute to the improvement of the SME for the following reason. If the  $\epsilon \rightarrow \gamma$  reverse transformation occurs over a wider temperature range and varies from place to place possibly from grain to grain, the local reverse transformation upon heating will exert internal stress in the neighbouring grains, resulting in the introduction of unrecoverable plastic deformation. This type of inhomogeneity would certainly be suppressed by simple thermal cycles or by deformation–heating cycles as observed in the present study. In the case of bending tests, the above-mentioned effect of homogenization

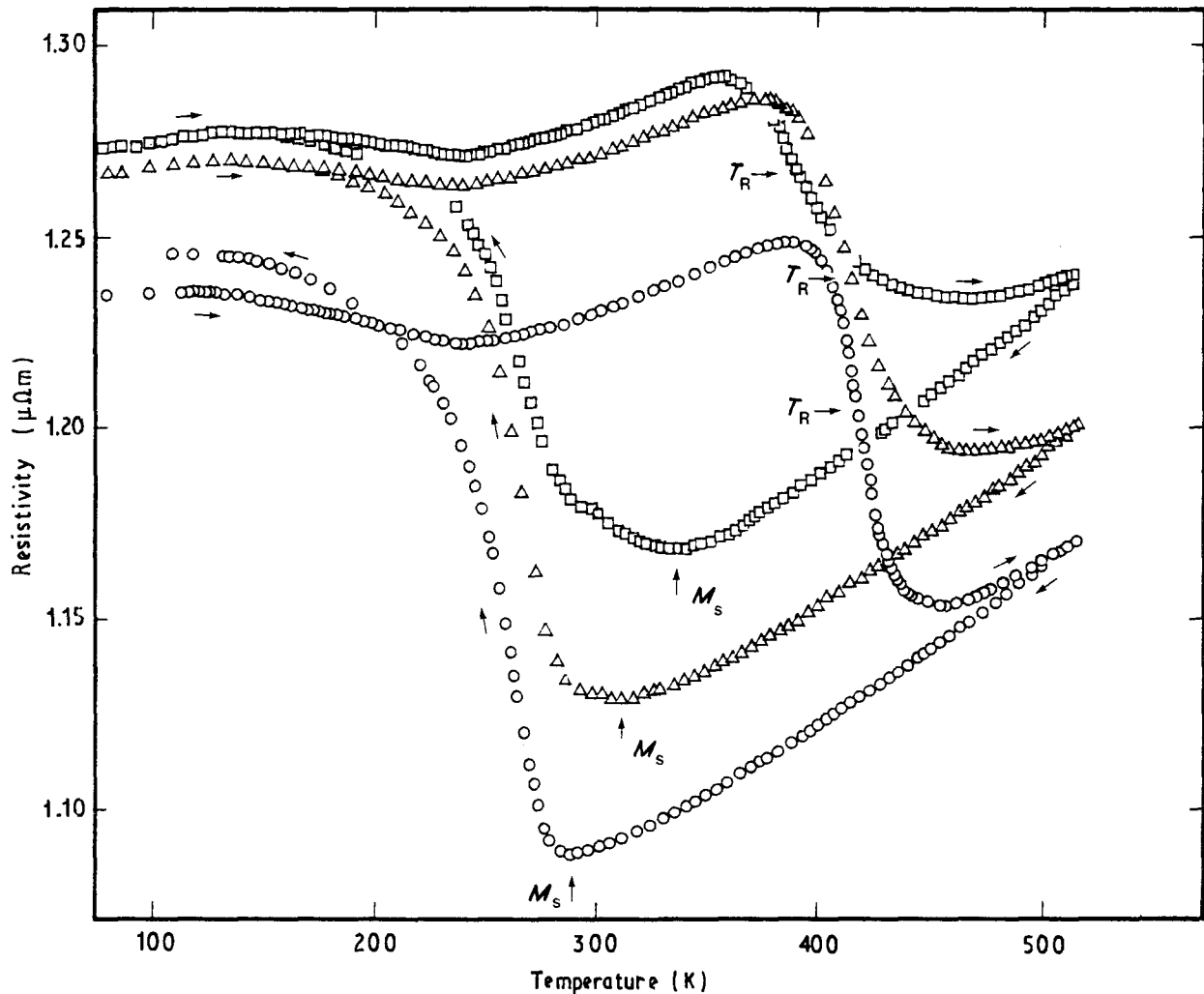


Figure 7 Electrical resistance versus temperature curves for a polycrystalline Fe-30 wt% Mn-6 wt% Si alloy. Run: (○) 1, (△) 8, (□) 14.

was noted visually as a rapid motion of the shape recovery upon heating.

Another effect of the thermal cycles or deformation-heating cycles contributing to the better SME is the elimination of the pre-existing  $\epsilon$  martensites in either single crystals or as heat-rolled polycrystals. The large yield stress for the first test at room temperature shown in Figs 2 and 3 indicates the effect of the presence of  $\epsilon$  martensites after specimen preparation, as seen in Fig. 6. However, they disappear after the deformation-heating cycles, indicating that development of a new structure by the training cycles involves the introduction of favourable  $\epsilon$  variants and elimination of unfavourable ones for the SME. The situation may be similar in polycrystals prepared by rolling at elevated temperatures.

If the observed refinement in the morphology is ascribed to the increase in the number of partial dislocations under operation, the temperature shift found in Fig. 4 can be explained as due to the change in the pre-exponential term in a rate equation. Representing the pre-exponential term before and after the training cycles by  $A_1$  and  $A_2$ , we have

$$A_1 \exp\left(-\frac{E}{kT_{R1}}\right) = A_2 \exp\left(-\frac{E}{kT_{R2}}\right) \quad (1)$$

where  $E$  is the activation energy for the partial disloca-

tion motion during reverse transformation,  $k$  is the Boltzmann constant,  $T_{R1}$  and  $T_{R2}$  are the temperatures dominant recovery before and after the training cycles, respectively. According to the previous study [1],  $E$  is found to be  $1.6 \times 10^{-19}$  J. When the pre-exponential term is related to the change in the number of mobile dislocations and hence change in the number of shear bands, Equation yields

$$N = \frac{A_2}{A_1} = \exp\left[\frac{E}{k} \left(\frac{1}{T_{R2}} - \frac{1}{T_{R1}}\right)\right] \quad (2)$$

where  $N$  indicates the increase in the mobile dislocation density. The above equation gives  $N = 8.4$  for  $T_{R1} = 420$  K and  $T_{R2} = 390$  K found in Fig. 4. In the actual observation, however, the increase in the number of  $\epsilon$  bands was  $\sim 50$  times at the fourteenth deformation cycle.

The underestimation of  $N$  in the above argument may, presumably, be ascribed to the over simplification, the constancy of  $E$ , adopted in Equation 1. If an expected decrement of a chemical driving force for partial dislocation motion at a lower temperature is taken into account, the above discrepancy will be resolved as follows. Assigning the energy change as  $\Delta E$  for the observed temperature shift, Equation 2 can be

modified to

$$N = \exp \left[ \frac{1}{k} \left( \frac{E}{T_1} - \frac{E + \Delta E}{T_2} \right) \right] \quad (3)$$

This equation gives  $\Delta E = 0.09 \times 10^{-19} \text{J}$  for the observed value of  $N = 50$ ,  $T_{R1} = 420 \text{ K}$  and  $T_{R2} = 390 \text{ K}$ . In the absence of accurate experimental data, the magnitude of  $\Delta E$  estimated above is in reasonable agreement with the temperature dependence of the chemical free-energy change associated with the  $\gamma \rightarrow \epsilon$  transformation obtained in the previous study [1]. It is, thus, gratifying that the observed temperature shift is well correlated with the structural change contributing to the training effect.

## 5. Conclusions

The origin of a training effect in an Fe–Mn–Si shape-memory alloy has been examined by length change and electrical resistivity measurements. The results of experimental findings are summarized as follows.

1. Deformation–heating cycles at a small strain causes irregular local deformation varying from place to place and changing from cycle to cycle, but resulting in homogenization and refinement of the structure after sufficient cycles.

2. The change in electrical resistivity of a polycrystalline alloy is shown to be well correlated with the observations on single crystals in describing the effect of training cycles on the transformation temperature and structural change.

3. A quantitative agreement is found between the structural change and the shift of reverse transformation temperature caused by the training cycles.

4. It is concluded from the above results that the training effect originates mainly from homogenization

of the deformation structure and removal of unfavourable  $\epsilon$  variants for the SME.

## Acknowledgements

This research was supported partly by a Grant-in-Aid for Scientific Research for the Ministry of Education and Culture (no. 63 430 045) and partly by Nippon Steel Corporation.

## References

1. A. SATO, E. CHISHIMA, K. SOMA and T. MORI, *Acta Metall.* **30** (1982) 1177.
2. A. SATO, E. CHISHIMA, Y. YAMAJI and T. MORI, *ibid.* **32** (1984) 539.
3. A. SATO, Y. YAMAJI and T. MORI, *ibid.* **34** (1986) 287.
4. M. MURAKAMI, H. OTSUKA, H. G. SUZUKI and S. MASUDA, in "Proceedings of the International Conference on Martensitic Transformations", (ICOMAT-86), Nara, Japan (The Japan Institute of Metals, Sendai, 1986) p. 985.
5. Y. HOSHINO, S. NAKAMURA, N. ISHIKAWA and A. SATO, in "Proceedings of the International Conference on Martensitic Transformations", (ICOMAT-89) (Trans. Tech., Brookfield, Vermont, 1990) p. 643.
6. T. A. SCHROEDER and C. M. WAYMAN, *Scripta Metall.* **11** (1977) 225.
7. L. CONTARDO and G. GUÉNIN, *Acta Metall.* **38** (1990) 1267.
8. H. OTSUKA, M. MURAKAMI and S. MATSUDA, Annual Meeting at Tokyo, *Jpn. Inst. Metals, Abstr. Bull.* **219** (1986).
9. M. MORIYA, H. SUZUKI, S. HASHIZUME, T. SAMPEI and I. KOZASU, in "Proceedings of the International Conference on Stainless Steels", Chiba (The Iron and Steel Institute of Japan, Tokyo, 1991) p. 527.

*Received 30 September 1991  
and accepted 11 August 1992*